Numerical and Experimental Assessment of Advanced Concepts to Reduce Noise and Vibration on Urban Railway Turnouts

Ioannis Anastasopoulos[1]; Stefano Alfi[2]; George Gazetas, M.ASCE[3]; Stefano Bruni[4]; and André Van Leuven[5]

Abstract: The short service life of rail turnouts and the related noise and vibration disturbance, are directly related to their dynamic distress. Especially in the case of urban rail systems, such problems are amplified due to the increased train frequency and the proximity to inhabited structures. This paper presents three new concepts for the reduction of noise and vibration produced by railway turnouts in urban railway lines, and provides an assessment of their performance. The effectiveness of the three new concepts is first evaluated analytically, using two different methodologies, earlier validated against line measurements on existing turnouts. Then, the actual performance of one of the three concepts, along with the effectiveness of the two analysis methodologies, is verified through real-scale measurements. Based on the presented analyses, all three new concepts are shown to provide a substantial enhancement of turnout performance. Furthermore, soil conditions and soil-structure interaction are shown to play an important role in the behavior of the investigated systems.

DOI: 10.1061/(ASCE)TE.1943-5436.0000007

CE Database subject headings: Dynamic analysis; Vibration; Soil-structure interaction; Maintenance; Noise control; Urban areas.

Introduction

Turnouts are used in railway networks to allow railway traffic being moved from one track to another where they intersect. They consist of three main components (Fig. 1): a switch panel where movable blades are used to control the direction of movement of the passing trains, the closure panel following the switch blades, and the crossing panel where the rails of the two tracks intersect at the same level.

The flange-way gap, necessary to provide wheel flange clearance at the point of rail intersection, is responsible for the development of large wheel impacts. Such dynamic loading is the main source of distress of turnouts, which explains why such systems often prove to be largely responsible for track failures, constituting one of the main causes of high maintenance costs. Furthermore, the sudden change of wheel-rail contact condition occurring across the flange-way gap is responsible for increased noise and vibration, so that turnouts usually represent the main source of vibroacoustic nuisance in urban railway lines, and have a relevant influence on public acceptance of new or existing urban rail networks.

This paper presents and evaluates the effectiveness of new turnout concepts for urban railway lines. Different means can be used to reduce impacts, noise, and vibration at turnouts, such as modifications of the nonuniform rail geometry along the crossing, improved control of rail surface wear, or the use of moveable point crossings (Esveld 1989; Giannakos 2000). However, the control of wear in urban lines is not easily applicable due to the high frequency of train passage; the use of moveable points is today confined to high-speed applications because of its substantial installation cost. Therefore, this work focuses on achieving improved vibration isolation through use of appropriate resilient and massive components in the track.

Hence, the following three new concepts for urban turnouts are considered in this paper:

1. A resilient track system, based on the traditional scheme of track over ballast, but improving the attenuation of noise and vibration through use of an under-sleeper and subballast elatomer mats, developed by D2S International;
2. A continuous rail support system, replacing ballast by a concrete slab foundation, developed by Kihn–Cogifer; and
3. A hybrid system using a mix of discrete and continuous rail supports, where the whole turnout is laid on an antivibratory concrete plinth, developed by Frateur de Pourcq (FDP).

These concepts are evaluated and assessed by a combination of numerical simulation and full-scale testing performed in the railway line.

The numerical evaluation is conducted using two different methods of analysis, earlier validated against line measurements on existing turnouts (Bruni et al. 2009). The first method focuses on wheel-track interaction, using a simplified finite-element model for the turnout structure; the second emphasizes modeling

[1]Adjunct Lecturer, School of Civil Engineering, National Technical Univ. of Athens, Athens 15780, Greece (corresponding author). E-mail: ianast@civil.ntua.gr

[2]Postdoctoral Researcher, Dept. of Mechanical Engineering, Politecnico di Milano, Milan, Italy.

[3]Professor, School of Civil Engineering, National Technical Univ. of Athens, Athens 15780, Greece.

[4]Professor, Dept. of Mechanical Engineering, Politecnico di Milano, Milan, Italy.

[5]Project Coordinator, D2S International, Brussels, Belgium.

Note. Discussion open until October 1, 2009. Separate discussions must be submitted for individual papers. The manuscript for this paper was submitted for review and possible publication on July 18, 2008; approved on November 3, 2008. This paper is part of the ***Journal of Transportation Engineering***, Vol. 135, No. 5, May 1, 2009. ©ASCE, ISSN 0733-947X/2009/5-279–287/$25.00.

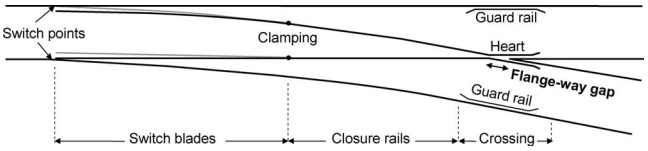

Fig. 1. Main components of a railway turnout

of the turnout structure and soil-structure interaction, incorporating a simplified model to compute the impact loading.

The experimental assessment (full-scale testing) is confined to the resilient track concept, for which results are available from tests comparing the vibration of nearby buildings, measured for a reference turnout on ballast and for the new turnout. These measurements allow a direct comparison, as they were performed on the same test site and using the same type of test vehicle.

The results presented in the paper provide evidence that all three new concepts are able to provide a substantial enhancement of turnout performance in terms of reduction of noise and vibration generated on the surrounding environment.

Three New Turnout Concepts

This section describes the main characteristics of the three new turnout concepts.

Resilient Track Concept

The resilient track concept aims at improving the filtering of mechanical vibrations provided by a standard turnout on ballast by the combined use of an under-sleeper mat and a subballast layer. A sketch of a typical section is represented in Fig. 2: the rails (in this case of the grooved type) are fastened to conventional sleepers laid on ballast, with an under-sleeper pad placed below the sleeper to increase resilience and damping at the sleeper-ballast interface. A ballast mat is then placed below the ballast as an interface with the track foundation and soil.

Given that this concept is developed for a tramway network, a concrete pavement is laid in between and aside the track, to provide a roadbed for the passage of road vehicles. To allow for relative movements between the track and the road, the rails are embedded by a filling material, and an interface layer is interposed between the concrete pavement and the sleepers.

Table 1 summarizes the stiffness (we use the term "stiffness" with its generalized definition, related to the modulus of the Winkler spring: $MN/m^3 = MN/m/m^2$ and damping parameters of the different resilient layers in the track: the sleeper-ballast interface (under-sleeper pad) and the ballast-soil interface (ballast mat). Stiffness data were obtained through laboratory measurements, while damping data were deduced from earlier measurements performed on similar elastomeric materials (Bruni and Collina 2000). Finally, the stiffness and damping parameters of the ballast layer are also reported in the table. These values were obtained on the basis of measurements on a conventional turnout system in the urban network of Brussels (through comparison of the computed and measured frequency response functions).

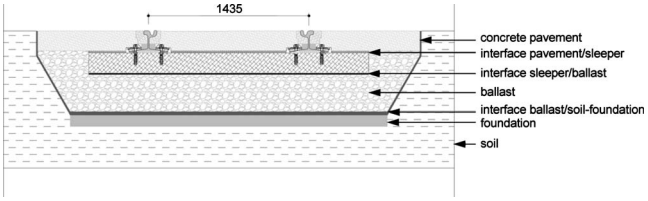

Fig. 2. Typical cross section of resilient track concept (developed by D2S)

Table 1. Stiffness Parameters of Different Resilient Layers in Resilient Track Concept, Developed by D2S

	Bulk modulus (MN/m^3)	Nondimensional dampling at 50 Hz
Under-sleeper pad	122	0.30
Ballast mat	50	0.30
Ballast	870	0.10

Continuous Rail Support Concept

In this concept, designed by Kihn–Cogifer, the turnout is mounted on a concrete slab replacing the ballast, while the rails are embedded into continuous rubber boots. The continuous rail support provided by the embedded rail system aims at reducing wheel-rail interaction and hence the emission of noise and vibration. The system was developed in two variants, one with a grooved rail with standard height (type NP4aS), the other with a low profile grooved rail (type 35GPB). Fig. 3 illustrates the Kihn–Cogifer turnout system during construction (in the case of standard height rail). The details of the embedded rail connection to the concrete slab and of the slab foundation can be observed.

Table 2 reports the nominal values for the stiffness (measured by lab tests) and damping (estimated) properties of the continuous rail support system. Additionally, the same table reports the stiffness and damping properties of a resilient layer which was intro-

Fig. 3. Continuous rail support system (developed by Kihn-Cogifer) during construction

Table 2. Stiffness Parameters of Different Resilient Layers in Continuous Rail Support Turnout System Developed by Kihn–Cogifer

	Stiffness per unit length (MN/m^2)	Nondimensional damping at 50 Hz
Continuous rail support layer	270	0.30
Slab-soil interface layer	760	0.30

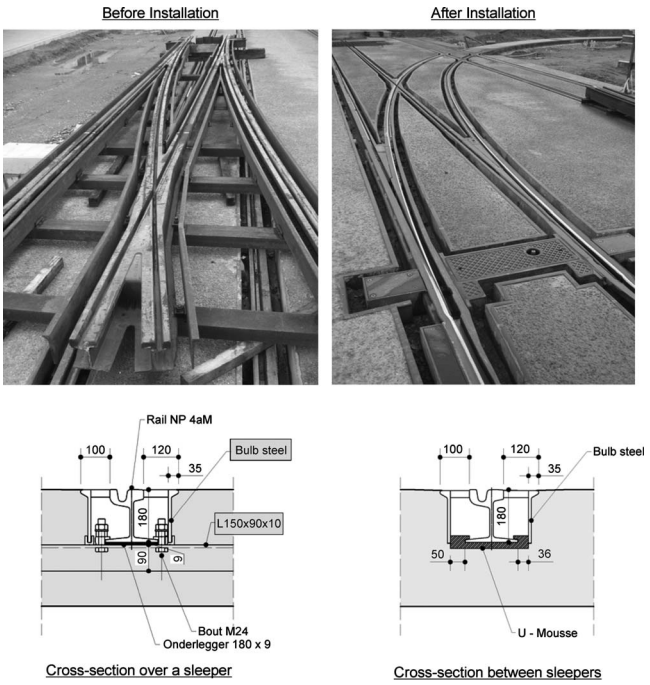

Fig. 4. Hybrid (continuous and discrete) rail support concept (developed by Frateur de Pourq) before and after installation, along with drawings of typical rail cross sections

duced in the mathematical models between the slab and the soil to account for local deformability effects occurring at the interface between the slab and the foundation.

Hybrid (Continuous and Discrete) Rail Support Concept

The third concept considered (designed by FDP) is based on the combined use of discrete and continuous rail support. To reduce noise and vibration transmission, the turnout is laid on an antivibratory concrete plinth. The rails (grooved type) are connected by fasteners to steel sleepers and enclosed between steel plates. Concrete is then poured around rails and sleepers to form the plinth, and finally the space left aside the rails is filled with resilient material. Between the sleepers, the rail rests on a continuous rail support provided by a rubber boot.

Fig. 4 depicts a prototype of this concept, before and after installation, and the connection between the rails, the concrete plinth, and the sleepers in two typical sections: over one the sleeper and inbetween the sleepers. Table 3 reports the nominal values for the stiffness and damping properties of the discrete fastener connecting the rails to the sleeper, and of the distributed layers realizing the continuous rail support and the slab/soil interface.

Table 3. Stiffness Parameters for Continuous and Discrete Rail Support Concept Developed by Frateur de Pourq

	Total stiffness per 0.6 m length (MN/m)	Stiffness per unit length (MN/m^2)	Nondimensional damping at 50 Hz
Fastener	200	—	0.30
Continuous rail support layer	—	30	0.30
Slab-soil interface layer	—	760	0.30

Methods of Analysis

Two different methodologies are used to perform the numerical assessment of the new turnout concepts: the first method focuses on wheel-track interaction, using a simplified finite-element model for the turnout structure, whereas the second one emphasizes the turnout structure and soil-structure interaction effects, applying a simplified model to compute impact loading due to wheel passage. Both methods are described in detail in Bruni et al. (2009), along with their validation through comparison with line measurements on existing turnouts. Hence, only a brief summary of the two methodologies is described herein.

Description of Method 1: Multibody Model

Focusing on wheel-track interaction, the first method is based on the coupling of a multibody model (Shabana 1989) of the entire train set and a finite-element model of the track. The train set is decomposed into several modules (Alfi and Bruni 2009), representing car bodies and bogies, and for each module the equations of motion are written with respect to a local moving frame traveling along the ideal path of the module, defined by the geometry of the line.

The equations of the train set are linearized (with respect to kinematic nonlinear effects only), assuming the motion to be a small perturbation around the large motion of the moving reference. For car bodies and bogie frames, a rigid body motion with constant forward speed is assumed, introducing 5 degrees of freedom per body. For the wheel sets, a flexible body description based on modal superposition is introduced (Diana et al. 1998).

The finite-element model of the turnout includes switch, closure, and crossing panels, along with two sections of standard track before and after the turnout to establish proper boundary conditions. Euler–Bernoulli beam elements are used to model the rails. Concrete slabs are modeled with plate elements and embedded rails by a distributed viscoelastic layer acting in vertical and lateral directions. A simplified representation of track foundation flexibility is included in the model by means of an equivalent beam resting on a viscoelastic layer.

The equations of motion for train and track are written separately, with wheel-rail contact forces acting as the coupling terms between the two sets of equations, requiring simultaneous solution of train and track equations. Due to the nonlinear effects associated with wheel-rail contact and to the nonlinear elements in the vehicles' suspension, the problem is solved in the time domain, using Newmark's implicit scheme modified according to Argyris and Mlejnek (1991) to introduce an iterative correction in the time step.

Wheel-rail contact forces are defined using a multi-Hertzian approach, where the formation of multiple contacts between each wheel and the rails may be reproduced. A detailed description of the general procedure for calculation of wheel-rail contact forces has been reported in Braghin et al. (2006). However, several specific effects were included in the model to account for the specific situation of turnout negotiation. More details can be found in Bruni et al. (2009) and Alfi and Bruni (2009).

Description of Method 2: 3D Finite-Element Model

The second method emphasizes on the turnout structure and soil-structure interaction effects, applying a simplified model to compute the impact loading. Each turnout is modeled in realistic detail using a three-dimensional (3D) finite-element model, which incorporates the whole turnout, comprising sleepers, rails, concrete plinths, isolating materials, etc. Numerical analyses were conducted utilizing the finite-element code ABAQUS (2004). All components are modeled through 3D hexahedral brick elements.

A composite boundary is introduced to incorporate the effect of neighboring sleepers, as well as of the longitudinal continuation of the rails. Thus, waves propagating longitudinally through rails are allowed to realistically radiate out of the 3D model, without spuriously affecting its performance. The same holds for vertically propagating waves.

A simplified analytical method [described in detail in Anastasopoulos and Gazetas (2007) and Bruni et al. (2009)] is developed to estimate the dynamic loading onto the turnout. Assuming that the wheels and turnout are subject to a degree of wear, and therefore their geometry is not ideal, wheel passage over the turnout is assumed to be dominated by "jumps" and impacts of the wheels while passing over the crossing nose of the turnout, instead of a smooth transition. The simplified analytical method simulates the impact of the wheel at the area of the crossing. All other wheel-track interaction phenomena are not considered.

The impact velocity of the wheel, as well as the impact point on the turnout, are computed applying the above mentioned analytical procedure. The model takes into account the primary suspension characteristics, the wheel mass, the total weight, and the running velocity of the vehicle, and the degree of relative wear of the wheels of the vehicle and running surfaces of the turnout. This way, the loading onto the turnout is an impact velocity and not a contact force, allowing the whole system to dynamically respond in a natural way.

Numerical Assessment of New Turnout Concepts

The two numerical simulation methods are used to assess the performance of the new turnout concepts. The assessment is performed considering a service condition where the turnout is installed in a tramway network and is negotiated by a six-axle articulated tramcar traveling at 25 km/h. Benefits brought by the new concepts are evaluated against a traditional turnout on ballast of the type installed in the STIB tramway network in Brussels, which is hereafter called the "reference" turnout. Rail accelerations and soil vibration under the turnout are taken as the key parameters to evaluate the performance of the considered turnout systems.

Performance of Resilient Track Concept

The 3D finite-element model (Method 2) of the resilient turnout concept by D2S is presented in Fig. 5. The model incorporates the various layers of the system, as realistically as possible. The dynamic response of the new concept turnout is first investigated parametrically, using Method 2, to highlight the effect of the governing parameters. Based on the specifications of the materials to be used in the new turnout, the following parameters were investigated:

1. Epoxy rubber stiffness and material damping:
   - $E_{epoxy}=4-20$ MPa; and
   - $\xi_{epoxy}=2-10\%$.
2. Ballast stiffness and material damping:
   - $K_{ballast}=35-70$ MN/m^3; and
   - $\xi_{ballast}=2-5\%$.
3. Ballast-mat stiffness:
   - $E_{balmat}=0.75-1.5$ MPa.
4. Subsoil stiffness, covering a reasonable range, from resilient to rigid foundation:
   - $K_{subsoil}=500-3{,}500$ MN/m^3.

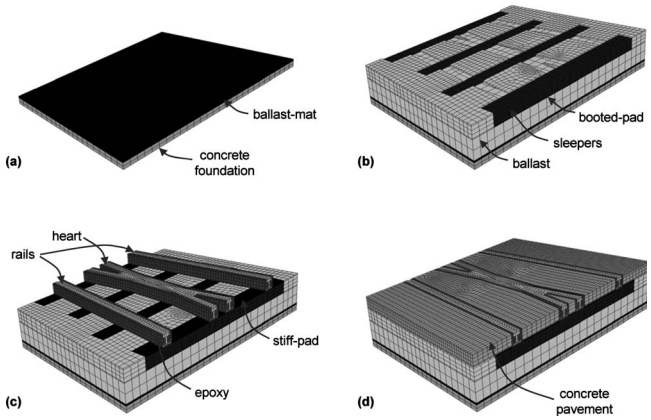

Fig. 5. Finite-element model (Method 2) of resilient track concept (D2S)

Dynamic analysis results (using Method 2) are illustrated in Figs. 6–8, in terms of vertical acceleration at characteristic points of interest: *A*, *B* along the crossing nose of the turnout (*A* close to the impact; *B* at a distance), *C* on the concrete pavement, *D* on the adjacent rail, and *E* just above the ballast mat.

The effect of epoxy rubber stiffness, E_{epoxy}, is summarized in Fig. 6. The increase of E_{epoxy} (from 4 to 20 MPa) leads to the decrease of the maximum vertical acceleration, a_{max}, along the crossing nose. In contrast, a_{max} on the concrete pavement is increased with E_{epoxy}. However, in all cases, the differences are only minor. Observe the dissipation of a_{max} along the surface of the turnout. While at point *A* (on the crossing nose, close to impact) a_{max} reaches 3–3.4 *g*, at point *B* (also on the crossing nose, but at a distance) a_{max} is reduced to 2.2–3 *g*. More importantly, a_{max} does not exceed 1 *g* at point *C*, on the pavement. It can be inferred that the pavement is effectively isolated from the vibrations of the crossing nose.

Fig. 7 illustrates the effect of ballast mat stiffness, E_{balmat}. At point *A* (crossing nose, close to the impact), the increase of E_{balmat} does not alter a_{max}. At point *D* (rail), the increase of E_{balmat} leads to a decrease of a_{max} from 1.3 to 1.1 *g*. Its effect is definitely more pronounced in depth: at point *E* (just above the ballast mat), the increase of E_{balmat} from 0.75 to 1.5 MPa, leads to a reduction of a_{max} from 2.1 to 1.2 *g*. This substantial effect can be attributed to wave reflection.

The effect of subsoil stiffness is illustrated in Fig. 8, varying $k_{subsoil}$ from 500 to 3,500 MN/m^3. While the first case is representative of a medium dense foundation soil, the second practically refers to a rigid subbase. The increase of $k_{subsoil}$ increases a_{max} at point *A* (crossing nose) from 3.2 to 4 *g*. Differences are not that significant on the rail (point *D*). As it would be expected, at point *E* (just above the ballast mat, and very close to the subsoil interface) a_{max} is significantly affected by $k_{subsoil}$. While in the case of the rigid subbase ($k_{subsoil}=3{,}500$ MN/m^3) a_{max} tends to zero (emitted waves cannot "penetrate" the rigid interface), with

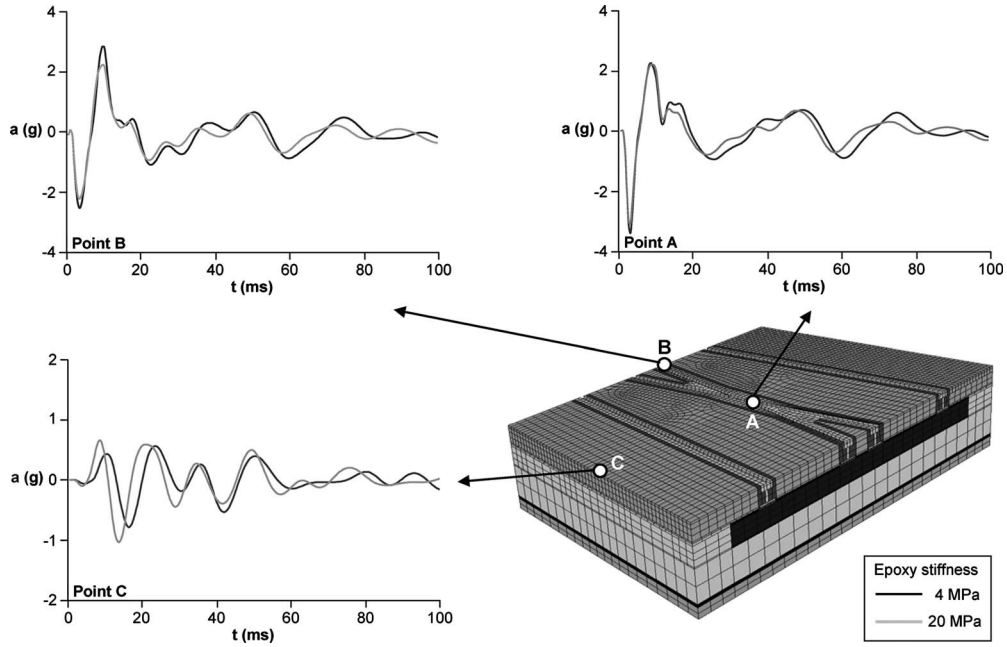

Fig. 6. Resilient track concept (D2S)—effect of epoxy rubber stiffness: acceleration time histories (using Method 2) at characteristic points of interest

$k_{subsoil}=500$ MN/m^3, a_{max} is substantially larger (of the order of 0.5 g). However, even in this case, the vibration is successfully absorbed by the system: a_{max} is reduced from 4 g at point A (close to the impact) to only 0.5 g at depth (point E).

Then, Method 1 is used to compare the performance of the new concept turnout to the reference turnout. Fig. 9 compares the 1/3 octave band levels of rail vertical vibration on the crossing nose (ref. 1e-9 g) for the reference turnout and for the resilient track concept (using Method 1). Rail vibration levels in the low-frequency range (below 40 Hz) are higher for the resilient track concept than for the reference track, whereas in the higher frequency range rail vibration levels are slightly lower for the D2S track, so that the overall RMS value is slightly reduced with the new concept, as reported in Table 4.

Such a slight performance amelioration is not relevant in view of turnout performance, however, the principal aim of the resilient track concept is to reduce vibration transmitted through the soil rather then rail vibration. If soil vibration is considered, the im-

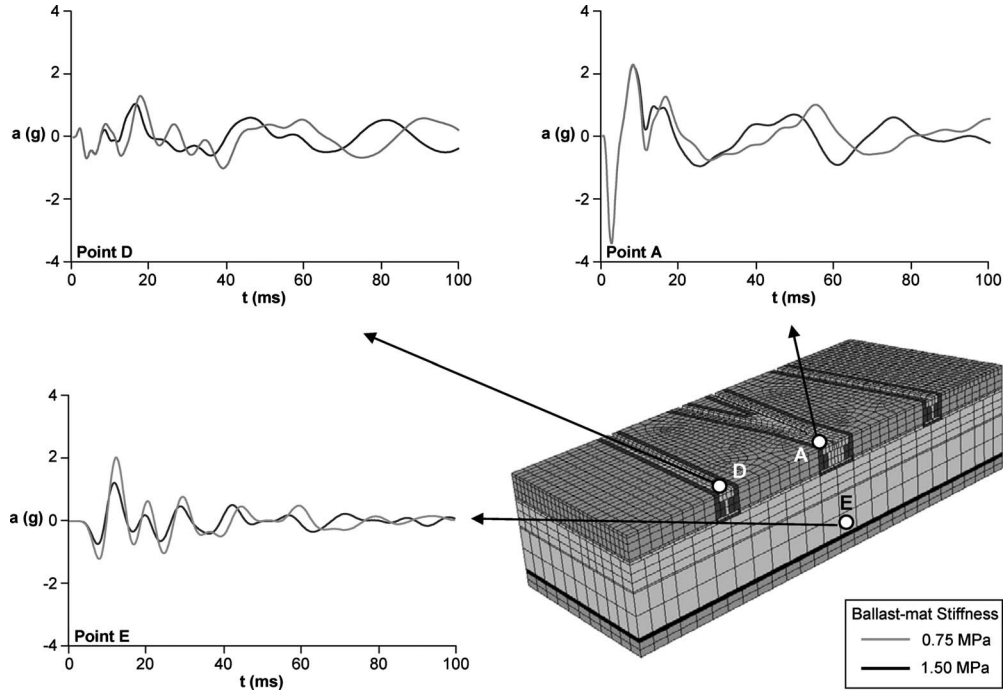

Fig. 7. Resilient track concept (D2S)—effect of ballast mat stiffness: acceleration time histories (using Method 2) at characteristic points of interest

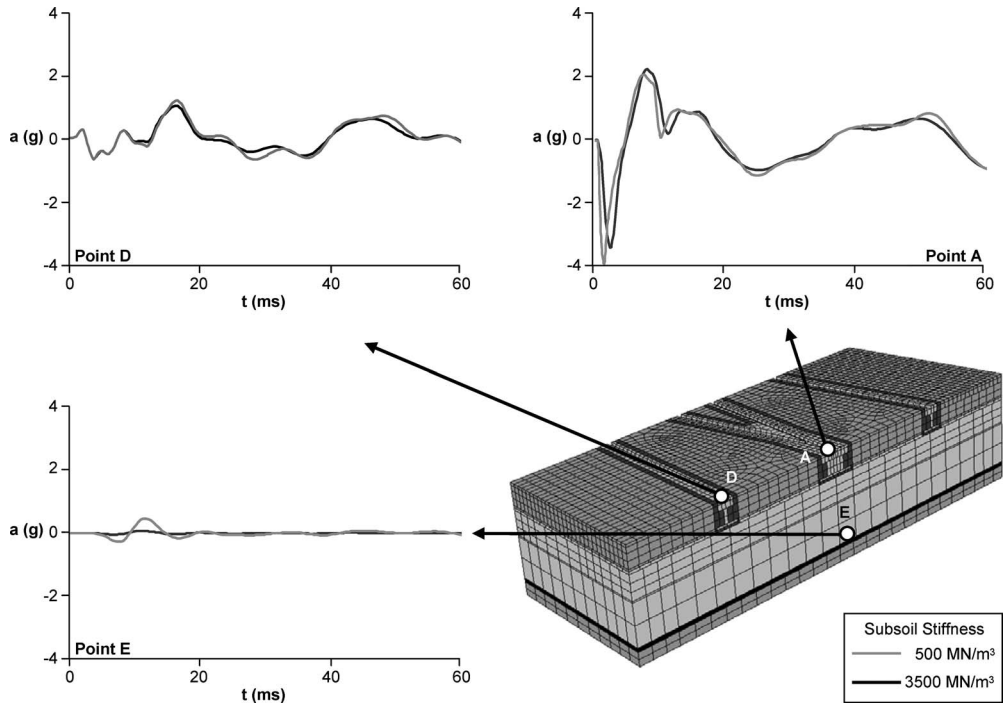

Fig. 8. Resilient track concept (D2S)—effect of subsoil stiffness: acceleration time histories (using Method 2) at characteristic points of interest

provement provided by the resilient track concept is easily recognized: Fig. 10 compares the numerically predicted vertical soil acceleration for the reference turnout and for the new concept. It is observed that above 40 Hz the resilient track provides a remarkable reduction of soil vibration, in the range of −10 dB or more.

This is a satisfactory result, because the higher levels of soil vibration occur between 50 and 200 Hz, and hence a relevant reduction of soil vibration may be achieved by this concept, as is also attested in Table 4, where an overall reduction of −9.6 dB of the RMS soil vibration is shown. This result is supported by experimental evidence obtained from line tests performed on the STIB network in Brussels, where a prototype of the resilient track concept was tested. Details of experimental results are provided in the sequel.

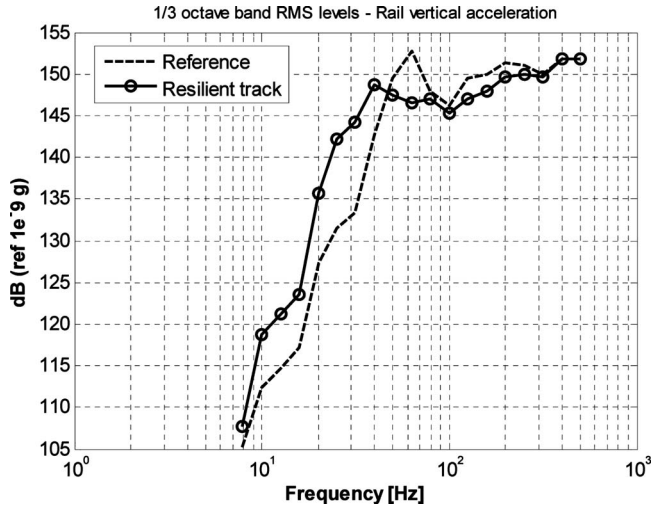

Fig. 9. Resilient track concept (D2S)—comparison of RMS vibration levels with reference turnout: vertical rail acceleration on crossing nose (results from simulation Method 1)

Performance of Continuous Rail Support System of Kihn–Cogifer

The 3D finite-element model (Method 2) of the continuous rail support turnout concept is illustrated in Fig. 11, incorporating the various components of the system, as realistically as possible.

As for the previous case, the dynamic response of the new concept turnout was first investigated parametrically, using Method 2, to gain insight into the sensitivity of the system to its prevailing parameters. Taking into account the properties of the materials that will be used in the new system, the following parameters were parametrically investigated:

1. Epoxy rubber stiffness and material damping:
   - E_{epoxy}=4–20 MPa; and
   - ξ_{epoxy}=2–10%.
2. Subsoil stiffness, covering a reasonable range, from resilient to rigid foundation:
   - $K_{subsoil}$=500–3,500 MN/m^3.

Table 4. Resilient Track Concept: Reduction of RMS Vibration Levels on Rails (Crossing Nose) and within Bearing Soil (Results from Simulation Method 1)

	Reference turnout RMS (m/s^2)	New concept RMS (m/s^2)	Reduction of vibration level (dB)
Vertical rail acceleration on the crossing nose of the turnout	1.12	1.00	−1.0
Vertical acceleration within the soil under the crossing	0.15	0.05	−9.6

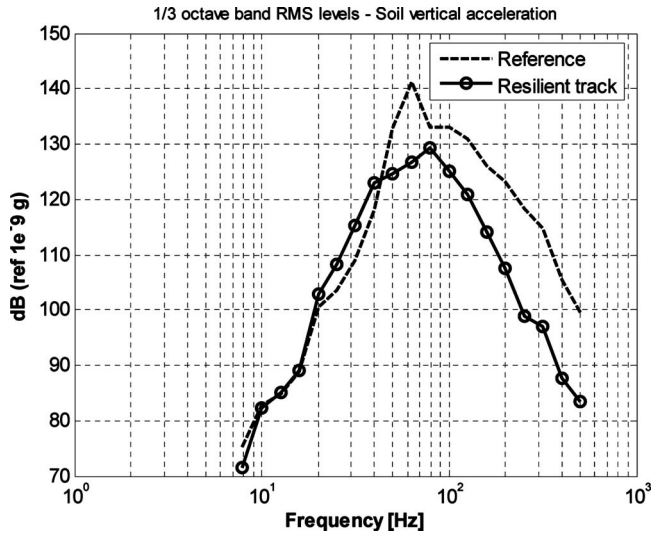

Fig. 10. Resilient track concept (D2S)—comparison of RMS vibration levels with reference turnout: vertical acceleration of soil under crossing (results from simulation Method 1)

In all cases examined, adjacent rails and concrete pavement are effectively isolated from the vibrating crossing nose of the turnout. As with the D2S concept, the increase of epoxy rubber stiffness leads to a decrease of the maximum vertical acceleration, a_{max}, along the crossing nose of the turnout, and to a slight increase on the concrete pavement.

Fig. 12 illustrates the effect of subsoil stiffness (for $E_{epoxy}=20$ MPa), in terms of vertical acceleration at characteristic points of interest E close to the impact area, F close to the rail, and G further away. The vertical acceleration on the pavement is reduced substantially with the increase of $k_{subsoil}$. At point E, a_{max} is decreased from 1.6 g ($k_{subsoil}=500$ MN/m^3) to 0.45 g ($k_{subsoil}=3{,}500$ MN/m^3). At all other points of interest (F,G), the increase of $k_{subsoil}$ leads to a dramatic decrease of a_{max}, which practically becomes zero with $k_{subsoil}=3{,}500$ MN/m^3.

As for the previous case, Method 1 is used to compare the performance of the new concept to the reference turnout. The continuous rail support incorporated in the new concept provides a spatially uniform impedance of the rail, reducing wheel-rail interaction in the mid- and high-frequency range. This results in a decreased level of rail vibration in the frequency range 40–200 Hz, as shown in Fig. 13, where rail vibration levels are compared for the reference and new concept turnouts, using a one-third octave band representation. In terms of RMS, the overall reduction of rail vibration is −3.5 dB (see Table 5).

The new concept also provides satisfactory performance in view of the reduction of soil vibration, as depicted in Fig. 14, where soil vibration levels under the turnout are compared for the reference and new turnouts. The continuous rail support (responsible for the reduction of crossing nose vibration levels), combined with the increased inertial impedance of the concrete slab, together allow for a substantial reduction of soil vibration levels in the frequency range above 50 Hz. For some of the one third octave bands, the reduction of soil vibration with respect to the reference exceeds 10 dB. In terms of RMS values, an overall reduction by more than 6 dB is achieved (see Table 5).

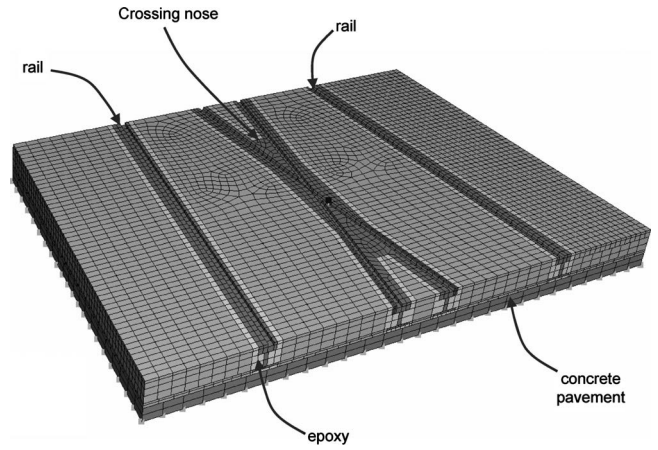

Fig. 11. Finite-element model (Method 2) of continuous rail support system (Kihn–Cogifer)

Performance of Hybrid (Continuous and Discrete) Rail Support Concept

The same assessment procedure was performed for the hybrid rail support concept. The results, not shown in detail for the sake of brevity, clearly demonstrate the effectiveness of the concept. The large inertia of the antivibratory plinth on which the new concept turnout is laid (see Fig. 4) allows for a reduction of rail vibration over the whole frequency range, resulting in a −5 dB reduction of the overall RMS level of rail vibration, as listed in Table 6. Soil vibration below the crossing is also reduced substantially, especially around 60 Hz, which corresponds to a resonance for the reference track. The reduction of the overall RMS value of soil acceleration is in the range of −6.5 dB (see Table 6).

Real-Scale Assessment of New Concepts

Prototypes of the three new turnout concepts were installed in urban railway networks to verify their performance through real-scale measurements under typical service conditions. This section presents characteristic results of such real-scale measurements, focusing on the resilient track concept for which results are available at the same site for a standard turnout on ballast, which was then replaced by the prototype of the new concept turnout. This allows for a direct comparison of their vibratory performance, since all testing conditions (including the service conditions, the soil parameters, etc.) are exactly the same for the reference and the prototype of the new concept turnout.

Tests were performed on the STIB tramway network in Brussels, where a complete prototype of the resilient track turnout with under-sleeper pads and ballast mat was installed in rue G. J. Martin. The tests were conducted on a standard turnout on ballast (August 2004), and later on an installed prototype of the new concept (February 2006). In both cases, soil acceleration measurements were taken at three different locations, named hereafter $P2$, $P3$, and $P4$. Position $P2$ was on the sidewalk running aside the tramway line, whereas positions $P3$ and $P4$ were established at two different locations in the foundation of a nearby building.

For the flexible track concept, Fig. 15 compares the one third octave band spectrum of the measured soil velocity at the three measuring locations [Fig. 15(a)] with the results of simulation for the same turnout concept [Fig. 15(b)], obtained using Method 1. Since the simulation method only includes a simplified representation of soil flexibility (soil is represented as a beam resting on a viscoelastic foundation), a quantitative comparison of the two re-

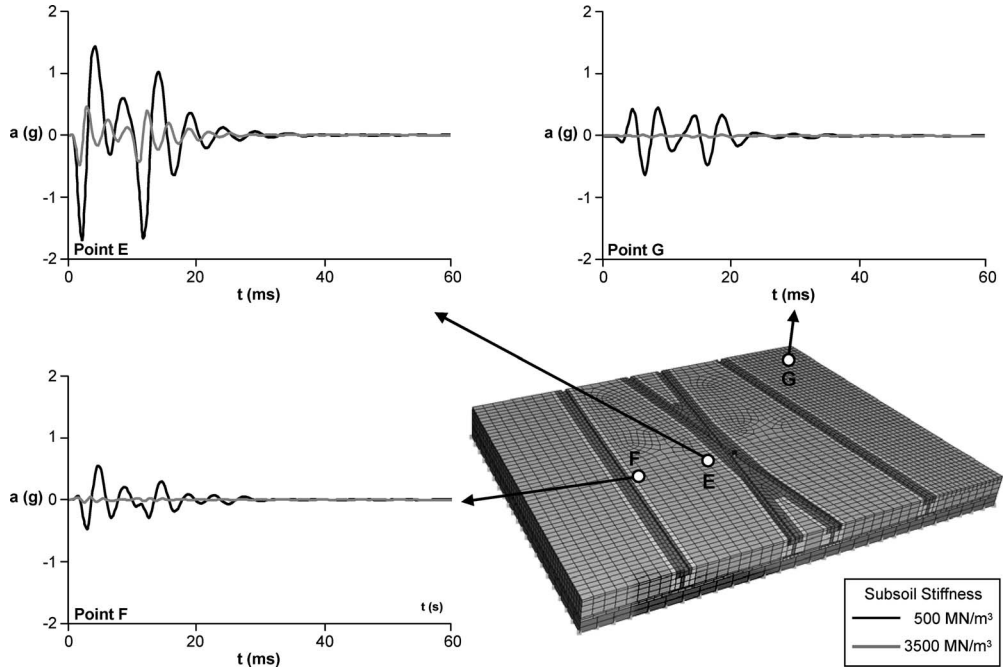

Fig. 12. Continuous rail support system (Kihn–Cogifer)—effect of subsoil stiffness: acceleration time histories (using Method 2) at characteristic points of interest

sults is not possible. However, a satisfactory qualitative agreement is found, with the measured and simulated soil velocity levels showing a similar trend with frequency, characterized by larger levels of vibration in the 30–100 Hz frequency range, and by decreasing levels of vibration at higher frequencies.

Table 7 compares the overall RMS levels of the measured soil velocity before and after installation of the new turnout prototype for the three measuring locations. To reduce the effect of measuring uncertainty, the results shown herein are averaged on several test runs that were repeated under the same testing conditions. These results show that the installation of the resilient track turnout produces a reduction of soil vibration levels in the range of 5–11 dB, depending on the measuring location.

The experimental evidence presented herein is in good agreement with the previously presented numerical predictions, which showed a reduction of soil vibration by approximately 10 dB for this concept. This result underlines and confirms the possibility of using the simulation methods presented herein as predictive tools for the design and assessment of low vibration tracks and turnouts.

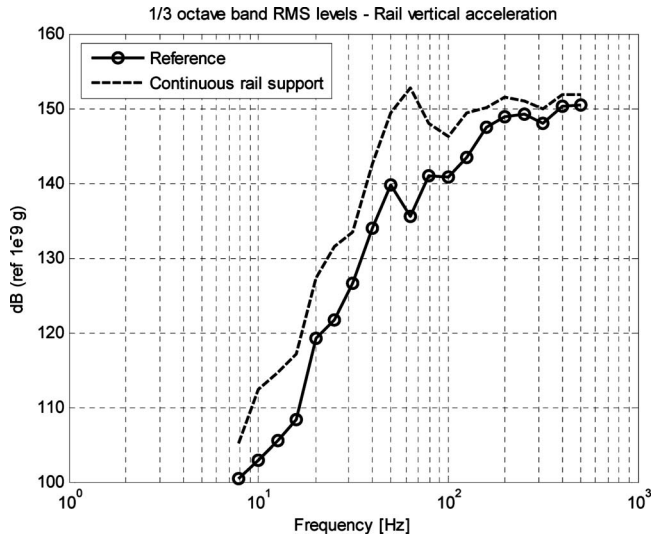

Fig. 13. Continuous rail support system (Kihn–Cogifer)—comparison of RMS vibration levels with reference turnout: vertical rail acceleration on crossing nose (results from simulation Method 1)

Conclusions

This paper has presented and evaluated the effectiveness of three new turnout concepts for urban railway lines, using two different analysis methods, earlier validated against line measurements on existing reference turnouts.

Results of numerical simulations show that the increase of track resilience of a turnout on ballast allows for a reduction of soil vibration in the range of −10 dB, whereas the levels of rail vibration are affected to a lesser extent. By introducing more radical changes in the design of the turnout, and in particular by using continuous rail support and a floating slab or an antivibra-

Table 5. Continuous Rail Support Concept: Reduction of RMS Vibration Levels on Rails (Crossing Nose) and within Bearing Soil (Results from Simulation Method 1)

	Reference turnout RMS (m/s^2)	New concept RMS (m/s^2)	Reduction of vibration level (dB)
Vertical rail acceleration on the crossing nose of the turnout	1.12	0.75	−3.5
Vertical acceleration within the soil under the crossing	0.15	0.07	−6.3

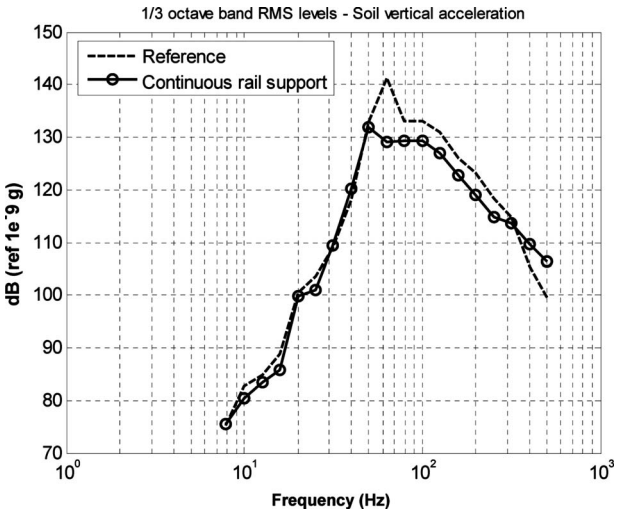

Fig. 14. Continuous rail support system (Kihn–Cogifer)—comparison of RMS vibration levels with reference turnout: vertical rail acceleration of soil under crossing (results from simulation Method 1)

Table 6. Hybrid (Continuous and Discrete) Rail Support Concept: Reduction of RMS Vibration Levels on Rails (Crossing Nose) and within Bearing Soil (Simulation Using Method 1)

	Reference turnout RMS (m/s^2)	New concept RMS (m/s^2)	Reduction of vibration level (dB)
Vertical rail acceleration on the crossing nose of the turnout	1.12	0.63	−5.0
Vertical acceleration within the soil under the crossing	0.15	0.07	−6.6

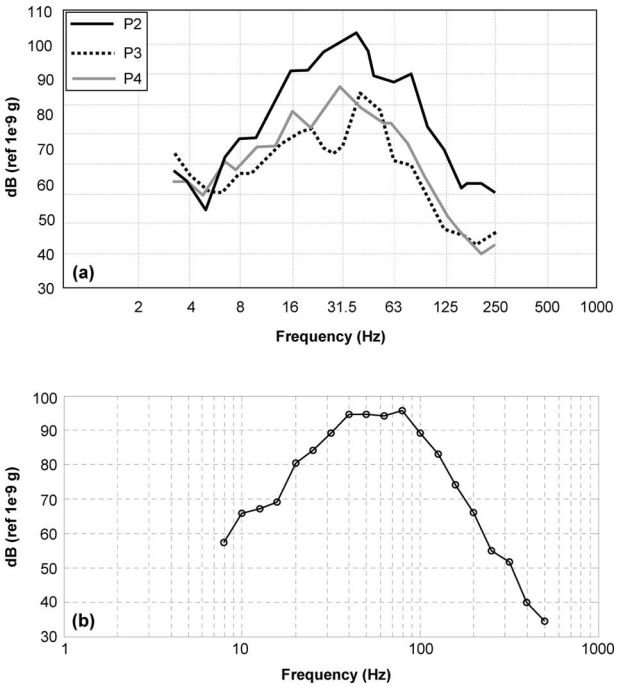

Fig. 15. Comparison of measured and simulated (using Method 1) soil velocity levels for resilient track turnout: (a) measured vibration at three different locations nearby; (b) simulation result (*P*2: on sidewalk running aside tramway line; *P*3 and *P*4: at two different locations in foundation of nearby building)

Table 7. Results of Line Measurements: Comparison of Measured RMS Soil Velocity for Reference Turnout and for Prototype of Resilient Track Concept

	Measuring location *P*2 (dB ref. 1e−9 m/s)	Measuring location *P*3 (dB ref. 1e−9 m/s)	Measuring location *P*4 (dB ref. 1e−9 m/s)
Average of measurements taken on the reference track	109.3	101.7	103.7
Average of measurements taken on the new concept	104.5	92.0	92.8
Reduction of vibration level	−4.8	−9.7	−10.9

tory plinth, it is also possible to considerably reduce the vertical vibration of the rails, which will result in reduced emission of air-borne noise.

Numerical results also show that subsoil conditions and soil-structure interaction play an important role in the overall response of the system investigated, and therefore antivibratory concepts should be designed considering the actual soil properties of the site where they are to be installed.

For one of the three new concepts, line measurements performed on an actual prototype confirm the findings of the numerical analyses presented herein, strengthening the validity of the derived conclusions.

Acknowledgments

The work presented in the paper was performed within the project "TURNOUTS," funded by the European Community (Contract No. TST3-CT-2003-505592).

References

ABAQUS, Inc. (2004). *ABAQUS V.6.4 user's manual*, Providence, R.I.

Alfi, A., and Bruni, S. (2009). "Mathematical modelling of train-turnout interaction." *Veh. Syst. Dyn.*, in press.

Anastasopoulos, I., and Gazetas, G. (2007). "Analysis of failure of scissors crossover guardrail support base-plates and the role of foundation-structure interaction." *Eng. Failure Anal.*, 14(5), 765–782.

Argyris, J., and Mlejnek, H. P. (1991). *Dynamics of structures*, North Holland, Amsterdam, The Netherlands.

Braghin, F., Bruni, S., and Diana, G. (2006). "Experimental and numerical investigation on the derailment of a railway wheelset with solid axle." *Veh. Syst. Dyn.*, 44(4), 305–325.

Bruni, S., Anastasopoulos, I., Alfi, S., Van Leuven, A., Apostolou, M., and Gazetas, G. (2009). "Effects of train impacts on urban turnouts: Modeling and validation through measurements." *J. Transp. Eng.*, submitted.

Bruni, S., and Collina, A. (2000). "Modelling the viscoelastic behaviour of elastomeric components: An application to train-track interaction." *Veh. Syst. Dyn.*, 34(4), 283–301.

Diana, G., Cheli, F., Bruni, S., and Collina, A. (1998). "Experimental and numerical investigation on subway short pith corrugation." *Veh. Syst. Dyn.*, 28, 234–245.

Esveld, C. (1989). *Modern railway track*, MRT-Productions, Duisburg.

Giannakos, C. (2000). *Actions on railway tracks*, Papazisi Publishers, Athens Geece (in Greek).

Shabana, A. A. (1989). *Dynamics of multibody systems*, Wiley, New York.